This article has been accepted for inclusion in a future issue of this journal. Content is final as presented, with the exception of pagination.

Small-Signal Stability Analysis of Large-Scale Power Systems in Response to Variability of Offshore Wind Power Plants

Amirhossein Sajadi, *Member, IEEE*, Shuang Zhao, Kara Clark, *Fellow, IEEE*, and Kenneth A. Loparo, *Life Fellow, IEEE*

***Abstract*—This paper presents a methodology for a small-signal stability analysis of large-scale power systems in response to variability of offshore wind power plants. This study considers the variability of wind power as the source of disturbance introduced to the system. To accomplish this goal, a singular value decomposition-total least squares extended Prony analysis is used to assess the small-signal voltage stability. In addition, a swing-based frequency response metric is used to assess the small-signal frequency stability. The case study here considers the integration of a 1000-MW offshore wind power plant, operating in Lake Erie, into the FirstEnergy/PJM service territory. This study uses a realistic model of the 63 000-bus test system that represents the U.S. Eastern Interconnection. The results verify the utility and practicality of this methodology for the integration studies of offshore wind power plants.**

***Index Terms*—Frequency response, offshore wind integration, power systems stability, small-signal stability, voltage stability.**

I. Introduction

SMALL-signal stability analysis of power systems addresses the dynamic behavior of such systems following small disturbances and assesses their capability to damp out the oscillations caused by disturbance [1]. A disturbance can include an expected or unexpected change in the level of power generation or consumption. In small-signal stability analysis, it is assumed that no contingency occurs and all of the grid's components are in normal operation.

Future power systems will be associated with a greater degree of volatility and complexity because of the involvement of renewable power generation sources and highly dynamic loads that will result in an overall change in the operating paradigm of power networks. Therefore, it is essential to develop relevant computational and analytical tools that are scalable and can be used to ensure the stability and operational security of electrical energy delivery in future systems [2]. The main objective of this paper is to tackle this problem.

The contribution of this paper is to introduce a comprehensive methodology for the assessment of small-signal stability of large-scale power systems in response to the variability of wind power generation as the disturbance to the system. This includes the areas of voltage stability analysis and frequency response. In practice, wind power usually changes with a moderate ramp. However, in severe cases, sudden changes as a result of wind gusts can force a sudden shutdown of the entire wind power plant or a part of it for safety reasons. Recently, wind gusts of up to 85 m/h forced dozens of wind turbines to shut down across the United Kingdom [3]. In this study, the disturbance to the system is modeled as an abrupt change in the level of wind power generation. Although, this study specifically addresses the offshore wind power plants, this methodology is generic and, therefore, practical for the planning and integration studies of renewable power plants of any form.

Voltage stability is a dynamic problem that can lead to voltage collapse if mismanaged [4]. For this class of stability analysis, modal analysis is often used to identify the full list of critical modes of the system including eigenvalue analysis [5]–[7]. The accuracy of modal analysis depends upon the accuracy of the system's model. Nonetheless, a detailed modeling of each of the system's components may result in a very large system matrix such that its eigenvalue decomposition can be time-consuming if at all possible. Thus, the eigenvalue analysis is not suitable for real-time power system analysis. Comparatively, Prony method is a very powerful technique for power system studies because it is able to monitor the linear behaviors of a nonlinear system that emerge from small-signal disturbances [8]–[11]. The first contribution of this work is to exploit singular value decomposition-total least squares (SVD-TLS) Extended Prony method to assess voltage stability directly from the time-domain voltage signals with a focus on the electromechanical modes. The SVD-TLS Extended Prony analysis does not require building power system models for performing linearization and implementing eigenvalue decomposition, which significantly reduces the workload and computational time.

Manuscript received April 2, 2018; revised August 22, 2018; accepted November 4, 2018. This work was supported by US Department of Energy under Grant DE–EE0005367: Great Lakes Offshore Wind: Utility and Regional Integration Study. The National Renewable Energy Laboratory's contribution to this work was supported by the U.S. Department of Energy under Contract No. DE-AC36-08GO28308 with NREL. The U.S. Government retains and the publisher, by accepting the article for publication, acknowledges that the U.S. Government retains a nonexclusive, paid-up, irrevocable, worldwide license to publish or reproduce the published form of this work, or allow others to do so, for U.S. Government purposes. *(Corresponding author: Amirhossein Sajadi.)*

A. Sajadi, S. Zhao, and K. A. Loparo are with the Department of Electrical Engineering and Computer Science, Case Western Reserve University, Cleveland, OH 44106 USA (e-mail: axs1026@case.edu; sxz119@case.edu; kal4@case.edu).

K. Clark is with the Power Systems Engineering Center, National Renewable Energy Laboratory, Golden, CO 80401 USA (e-mail: Kara.Clark@nrel.gov).

Digital Object Identifier 10.1109/JSYST.2018.2885302

1937-9234 © 2018 IEEE. Personal use is permitted, but republication/redistribution requires IEEE permission.
See http://www.ieee.org/publications_standards/publications/rights/index.html for more information.

Pursuant to the DOE Public Access Plan, this document represents the authors' peer-reviewed, accepted manuscript.
The published version of the article is available from the relevant publisher.

This article has been accepted for inclusion in a future issue of this journal. Content is final as presented, with the exception of pagination.

Frequency response is defined as the ability of power system to adequately manage its frequency regulation immediately after a disturbance takes place [12]. The frequency response of a power system is strongly dependent on the mechanical inertia of the generators and depends on the rotational kinetic energy that they can absorb and release [13]. With high penetrations of renewable energy units (solar panels and wind turbines), the calculation and computation of system inertia can be very complicated, and this has raised concerns about the frequency response of large-scale interconnected power systems. The second contribution of this work is to use a swing-based frequency response metric to assess small-signal frequency response of the system. The metric uses the peak-to-peak value of the frequency swing in time domain with respect to the amplitude of the disturbance.

This methodology is practical for transmission system planning studies for the integration of wind power plants into utility service areas. It offers a great utility and efficiency considering that it is 1) easy to implement on existing practical network models, 2) practical and useful with available power system simulation packages, 3) inherently including the effects of discontinuous system elements (such as controller limits or saturation effects), and 4) more computationally efficient than conventional analytical tools that have limited applicability to large and complex power systems.

The case study used in this research involves the integration of a 1000 MW offshore wind power plant operating in Lake Erie into the FirstEnergy/PJM service territory. A simulation model of the U.S. Eastern Interconnection is used as the test system, 63k-bus test system. This model is constructed in GE PSLF software package based on a previous work for the Eastern Frequency Response Study [15]. The previous databases are modified slightly from the Eastern Frequency Response Study [16] model based on recent changes to the available generation in the FirstEnergy system. Potential geographical locations of offshore plants and points of interconnection (POIs) are identified based on estimation of wind availability by the U.S. Department of Energy's National Renewable Energy Lab (NREL) [14]. Accordingly, relevant feasible integration scenarios are developed. The wind turbines are modeled as GE 3.6-MW commercial wind machines [17].

II. Methodology

Power systems are complex nonlinear dynamical systems that are meant to operate at a stable equilibrium or near it. However, following an external disturbance, the state of the system may change and tends toward an unstable equilibrium. Small-signal stability analysis tends to understand the behavior of the system around an equilibrium point and determine whether or not it is locally stable.

Following section describes a methodology for small-signal stability analysis associated with the integration of offshore wind power plants into large-scale power systems.

A. Voltage Stability

Voltage stability is a dynamic problem that can be exacerbated by the control actions of the generators, load dynamics, and on-load tap-changers and can lead to voltage collapse [4]. For small-signal voltage stability analysis, modal analysis is often used [5]–[7] . This approach relies on linearized dynamic models of individual electrical components of the system and is often impractical for large-scale interconnected power systems. For instance, the U.S. Eastern Interconnection model consists of approximately 63 000 buses. Roughly more than 20 000 of these buses are equipped with dynamic devices. Depending on the model, the number of state variables can range from 2 to 10 for any given device. In total, the overall number of state variables ranges from 40 000 to 200 000.

An alternative approach is the Prony analysis. The Prony method is a useful tool in studying system stability and dynamics because it identifies the amplitude, frequency, damping, and phase parameters of the system modes directly from the time-domain response data [9]. The Prony method models a measured data sequence as a linear combination of complex exponentials with damping [18]. The procedures can be summarized into three steps: 1) solve a set of linear prediction equations to obtain the coefficients that are used to form a linear prediction error polynomial; 2) obtain the frequency and damping estimates from the roots of the linear prediction error polynomial; and 3) compute the amplitude and phase estimates from the residues obtained by solving a Vandermonde problem.

This paper borrows the SVD-TLS Extended Prony method [19], [20] and exploits it to identify the dominant voltage modes directly from the voltage measurement signals. This method estimates the number of modes by either the effective rank [21] or the signal-to-noise ratio (SNR) criterion [8]. The advantage of the effective rank is that once it is correctly determined, the Prony algorithm only needs to be performed once to give the estimation. However, in the cases in which the energy of some modes are much smaller than others, the first a few largest singular values, which correspond to modes with large energy, are much larger than the rest of the singular values. Such that when the criterion is satisfied, the effective rank would be less than the actual number of modes and this results in inaccurate parameter estimation. The SNR criterion requires repetition of Prony analysis in each iteration starting from order 1 until the criterion is met. When the number of modes contained in the signal is large, the steps of Prony analysis would be repeated for a large amount of times, which increases the computational effort and time. Both criteria have been combined in the method used in this paper to find the estimated order. First, the effective rank criterion is used to find the initial order. Then, the order is updated until the SNR constraint is satisfied. Thereby, an appropriate estimated order can be obtained with less computational effort.

To examine the application of this method, a 3-machine, 9-bus test case [22], shown in Fig. 1, is used as a proof of concept. This test model is a benchmark model for the analysis and control of small-signal dynamics in power systems, and represents an approximation of the Western Electricity Coordinating Council. The disturbance examined in this case is a 40% increase of load connected to bus 5, from 90 to 125 MW. The results from modal analysis of this system are shown in Table I.

After modal analysis, the Prony analysis was applied to the voltage time-series signals to determine the dominant voltage

Pursuant to the DOE Public Access Plan, this document represents the authors' peer-reviewed, accepted manuscript. The published version of the article is available from the relevant publisher.

This article has been accepted for inclusion in a future issue of this journal. Content is final as presented, with the exception of pagination.

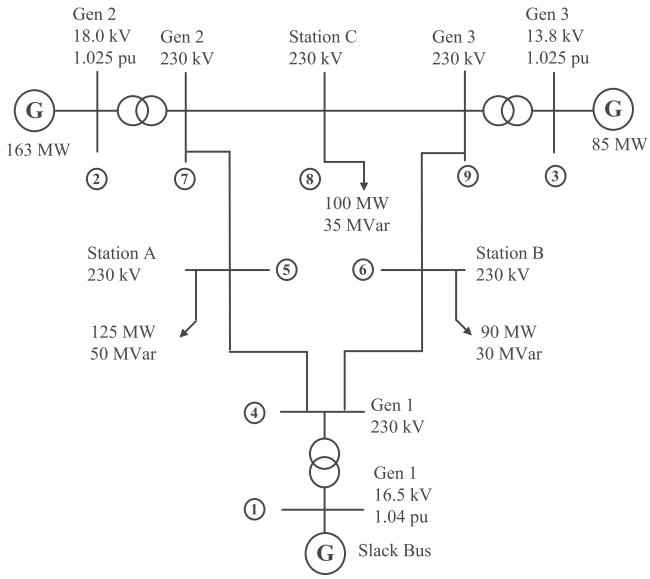

Fig. 1. One-line diagram of the WECC 9-bus test system [23].

TABLE I
EIGENVALUES OF TEST SYSTEM

Eigenvalue	Frequency	Damping Ratio	Machine Number
-0.82 $\pm$ j12.59	2.0 Hz	0.06	3
-0.50 $\pm$ j9.06	1.4 Hz	0.05	2
-5.16 $\pm$ j7.88	1.2 Hz	0.54	3
-5.16 $\pm$ j7.81	1.2 Hz	0.55	1
-5.15 $\pm$ j7.87	1.2 Hz	0.54	2
-0.09 $\pm$ j4.83	0.7 Hz	0.02	1
-0.43 $\pm$ j0.89	0.1 Hz	0.43	1
-0.40 $\pm$ j0.74	0.1 Hz	0.84	2
-0.41 $\pm$ j0.56	0.0 Hz	0.59	3

modes, magnitude, and damping ratio. The results are shown in Table II.

The Prony analysis yields that the dominant frequencies of the voltage modes are 1.3 and 0.1 Hz with damping ratios of approximately 0.05 and 0.43, respectively, as shown in Table II. These modes are consistent for all voltage signals, whereas the amplitude of the modes varies for each signal as they are dependent on the network topology. The modes identified by the Prony analysis are identical to those identified by the modal analysis, shown in Table I. As the load changes at bus 5, it triggers a set of changes in the dynamics of the machines that are connected to both ends of the lines (knowing that the small-signal disturbances are local events and trigger local responds). As a result, the dominant modes related to machine 1 and machine 2 are excited. It should be noted that the other modes, which are determined by the modal analysis but do not appear in the voltage measurements and, subsequently, are not identified by the Prony analysis, may appear in other state variables, for example, in rotor angle oscillation modes. Those modes do not have direct contributions to the voltage modal analysis.

The analysis on the test system demonstrated the application and accuracy of the SVD-TLS Extended Prony method for

TABLE II
RESULTS OF THE PRONY ANALYSIS ON VOLTAGE SIGNALS FROM THE TEST SYSTEM

Bus	Amplitude	Frequency	Damping Ratio
1	1.9×10^{-4}	1.3 Hz	0.05
	1.3×10^{-2}	0.1 Hz	0.43
2	7.6×10^{-4}	1.3 Hz	0.05
	2.2×10^{-2}	0.1 Hz	0.46
3	4.9×10^{-4}	1.3 Hz	0.05
	2.0×10^{-2}	0.1 Hz	0.45
4	6.2×10^{-4}	1.3 Hz	0.05
	1.5×10^{-2}	0.1 Hz	0.44
5	6.6×10^{-4}	1.3 Hz	0.06
	1.7×10^{-2}	0.1 Hz	0.46
6	7.5×10^{-4}	1.3 Hz	0.05
	1.6×10^{-2}	0.1 Hz	0.40
7	8.1×10^{-4}	1.3 Hz	0.05
	1.9×10^{-2}	0.1 Hz	0.44
8	8.0×10^{-4}	1.3 Hz	0.06
	2.1×10^{-2}	0.1 Hz	0.46
9	6.1×10^{-4}	1.3 Hz	0.05
	2.0×10^{-2}	0.1 Hz	0.45

the identification of voltage modes directly for the time-series voltage signals following a small disturbance. This finding is helpful for small-signal voltage stability analysis of large-scale power systems for which the modal analysis approach may be too computationally intensive or simply not possible to use.

B. Frequency Response

Frequency inertial response, often called by *Frequency Response*, refers to the response of the system to frequency changes without changing the governor's reference values. The time frame of this stage of frequency control is within the first few seconds following a disturbance [1].

The frequency dynamics of a multi-machine power system with m generators following a small disturbance could be expressed by

$$\frac{\Delta f_s}{\Delta P_{dist}} \approx \frac{f_s}{\sum_{i=1}^{m} H_i \cdot S_{n_i}} \tag{1}$$

where f_s is the area synchronous frequency, P_{dist} is the disturbance power, and H_i and S_{n_i} correspond to the inertia constant and nominal rated power of the ith generator. On one hand, according to (1), the frequency response of a system is highly dependent on the inertia of the system. On the other hand, the renewable energy systems such as solar panels and wind turbines are interconnected to the power systems through power electronic interfaces that are fully isolated or partially isolated from the system and, therefore, their inertia contribution is very limited or nonexistent [12]. Therefore, the integration of renewable energy systems can affect the system's frequency response.

The power industry uses frequency response metrics [15], [24], [25] to assess the frequency-related performance of an interconnected system in terms of MW/0.1 Hz [26]. These metrics relate the amount of lost generation to the resulting frequency drop in the system and use a variety of indicators such as the

Pursuant to the DOE Public Access Plan, this document represents the authors' peer-reviewed, accepted manuscript.
The published version of the article is available from the relevant publisher.

This article has been accepted for inclusion in a future issue of this journal. Content is final as presented, with the exception of pagination.

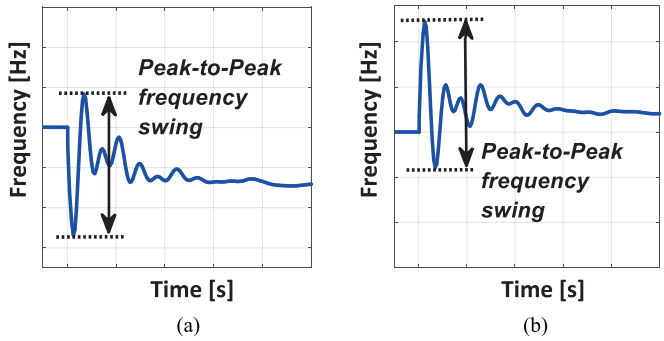

Fig. 2. Sample frequency profiles following wind intermittency. (a) Wind drop. (b) Wind rise.

nadir and settling frequency values with respect to the level of generation loss. Nonetheless, these metrics are incapable of fully capturing the dynamics of the system's frequency following local perturbations during which frequency overshoots may occur [27].

This paper assesses the frequency response of power systems as a result of the variability of offshore wind power plants. This include rise and drop of power generation that can result in frequency oscillations depending on the magnitude of wind intermittency. Specifically, this paper considers a peak-to-peak value-based frequency response metric for small-signal frequency response assessment. This metric quantifies the performance of power systems in response to disturbances introduced by intermittency of offshore wind power plants. Given a change in the level of wind power generation, the balance between generation and consumption in the system is disrupted and, hence, the frequency begins to fluctuate. This metric relies on quantifying the frequency swings that follow the disturbance, specifically the peak-to-peak frequency range as shown in Fig. 2.

As shown in Fig. 2, the area frequency inherently declines following a drop in wind power generation, while it rises following an ascent in wind power generation. Hence, the primary frequency response index (PFRI) is defined by

$$\text{PFRI} = \frac{\text{Change in Wind Power Generation } (MW)}{\text{Frequency Swing Level } \quad (0.1\text{Hz})}. \qquad (2)$$

The greater ability of the system to withstand changes in the level of wind power generation results in a smaller magnitude of observed frequency oscillations. Hence, the greater the value of PFRI, the stronger the frequency response of the system.

To examine the reliability and accuracy of this index for frequency response assessment of power systems, the PFRI value for the U.S. Eastern Interconnection is compared with the results from three other frequency response studies, which analyzed the same benchmark and were carried out by the U.S. Department of Energy's national laboratories: 1) the Lawrence Berkeley Lab (LBL) frequency response study in 2010 [25], 2) the GE and NREL frequency response study in 2013 [16], and 3) the Oak Ridge National Laboratory (ONL) frequency response study in 2015 [28]. The frequency response in this study is measured following the disconnection of a single 1000 MW unit generation unit in the FirstEnergy power area. The results are presented in Table III.

TABLE III
SUMMARY OF FREQUENCY RESPONSE FOR THE EASTERN INTERCONNECTION

Study	Frequency Response (MW/0.1Hz)
LBL	2,500
NREL	2,200
ONL	2,318
This study	2,272

Following the loss of a 1000 MW unit, the area frequency holds a peak value of 60.00 Hz with a nadir of 59.956 Hz, yielding a 0.044 Hz peak-to-peak value and, subsequently, the PFRI value of 2272. Accordingly, the quantification of the Eastern Interconnection's response using the PFRI is consistent with findings from the other studies as presented in Table III. This suggests that the PFRI is a reliable measure for the assessment of frequency response in power systems.

III. Case Study

The case study used in this paper considers the integration of a 1000 MW of offshore wind power plant in Lake Erie into the FirstEnergy/PJM transmission system. This section describes the details of the case study and the computational implementation of the small-signal stability methods proposed in this paper.

A. FirstEnergy/PJM Power System

In this study, a realistic computer model of the PJM power system is used. The PJM is a regional transmission operator in the Midwestern United States. It is part of the Eastern Interconnection and operates an electric transmission system. FirstEnergy is a regional utility company, based in Akron, OH, USA, within a geographical subregion of PJM and serves 6 million customers in Ohio, Pennsylvania, West Virginia, Virginia, Maryland, New Jersey, and New York.

B. Wind Power Integration Scenario Development

The estimated geographic distribution of available wind power over the surface of Lake Erie was provided by the NREL and based on these estimates, the candidate POIs were identified in the FirstEnergy transmission system. Accordingly, three scenarios for the integration of a total of 1000 MW of offshore wind generation, subject to compatibility with the extant grid infrastructure, were developed.

1) Interconnecting a total of 1000 MW of offshore wind generation at a single POI: 205-located at the Perry 345 kV substation, referred to as **EC01**.
2) Interconnecting a total of 1000 MW of offshore wind generation through the aggregate of five 200-MW connections at POIs across the lakeshore: 205-located at the Perry 345 kV substation, 214-located at the Ashtabula 138 kV substation, 225-located at the East Lake 345 kV substation, 234-located at the Lake shore 138 kV substation, and 245-located at the Avon Lake 345 kV substation, referred to as **EC02**.

Pursuant to the DOE Public Access Plan, this document represents the authors' peer-reviewed, accepted manuscript. The published version of the article is available from the relevant publisher.

This article has been accepted for inclusion in a future issue of this journal. Content is final as presented, with the exception of pagination.

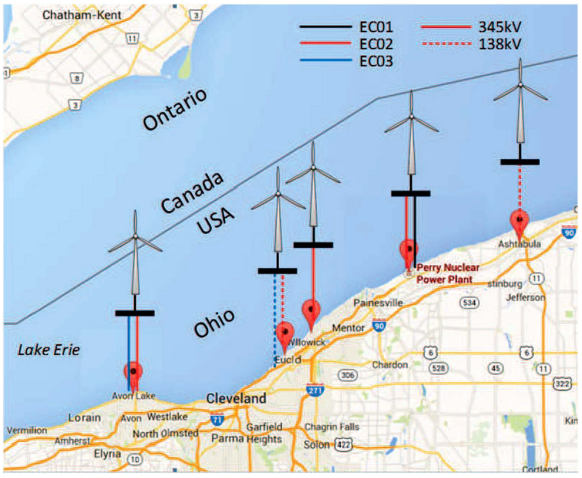

Fig. 3. Map of locations of the planned 1000 MW offshore wind power plant and candidate POIs.

3) Interconnecting a total of 1000 MW of offshore wind generation through the aggregate of two 500-MW connections at two POIs across the lakeshore: 234-located at the Lake shore 138 kV substation and 245-located at the Avon Lake 345 kV substation, referred to as **EC03**.

Fig. 3 shows the geographical locations of the POIs.

C. Offshore Wind Power Plant Model Development and Computer Modeling

For computational purposes, the 1000-MW offshore wind power plant is treated as a group of generators that are aggregated through a 34.5-kV collector system. Consequently, the outputs of each of these groups of generators are aggregated in an offshore collector system connected to a PV bus through medium voltage ac export cables. The wind turbine model parameters used in this study are based on a Type 3 GE 3.6-MW offshore wind turbine [17]. The parameters of the export cables that transmit the offshore power to onshore substations are designed and modeled based on the data from the ABB on commercial offshore cables [29].

Static VAR compensators (SVC) with significant compensation capacity were inserted at the POIs in the computer model. The levels of reactive power generated/consumed by the SVCs were monitored during simulation to determine the capacity of the compensation devices required for providing ancillary services to the grid. The dynamic models used to represent these devices are simple Static VAR devices, *VWSCC* in GE's PSLF model library [30]. The analysis considered a maximum/minimum SVC rating of ±500 MVar.

More information about these models is available in GE's PSLF documentation [30].

D. Generation Dispatch Scenarios and Load Assumptions

The main objective of this particular case study is to study the stability-related impacts of the integration of 1000 MW of offshore wind power generation into the FirstEnergy/PJM transmission system. To this end, the winter 2013 load data from the Eastern Interconnection were modeled in PSLF. The model contains 63 608 system buses and 8356 generators, with a total of 894 772 MW and 411 288 MVar of installed generation capacity to serve a load of 302 086 MW and 75 596 MVar.

Operational scenarios were developed to consider the impacts of the decommissioning of Perry, a 1200-MW power plant in the area, upon the integration of the offshore wind power plant. Subject to the operating status of Perry, generation units in the area were redispatched to maintain the balance between generation and consumption for each of the developed interconnection and operational scenarios.

E. Computer Implementation

The computer simulation was carried out using GE's PSLF Version 18.1 01 80 K, DYTOOLS simulation tool. Accordingly, four cases for each of the interconnections (EC01, EC02, and EC03) were developed.

1) *Case 1:* Perry online, SVC offline.
2) *Case 2:* Perry online, SVC online.
3) *Case 3:* Perry offline, SVC offline.
4) *Case 4:* Perry offline, SVC online.

After loading the steady-state models, generation dispatch, and load data, the wind models were initiated. The dynamic models of the system were then loaded, including detailed representations of generators and their control systems, stabilizers, governors, dynamic loads, and other dynamic components of the grid.

The main objective of this paper is to conduct a small-signal stability analysis for a large-scale power system in response to the variability of an offshore wind power plant. Therefore, step changes in power generation by the offshore wind power plant were introduced into the system. The sizes of the disturbances were determined to be consistent with the expected changes in wind power, estimated by the NREL: ±360, ±140, ±75, ±40, and ±30 MW. This estimation provided the necessary basis for choosing the pre-disturbance operating points for the offshore wind power plant to cover a realistic spectrum of possible intermittency scenarios with respect to the 1000 MW capacity. Hence, the offshore wind power plant was studied for multiple pre-disturbance operating points of the wind power plant, including 1000, 800, 600, and 400 MW.

The simulations were initiated for the first 5 s to settle startup transients. Then, the wind intermittency event took place at the fifth s and the dynamic simulations covered 20 s following the event (total of 25 s dynamic simulation for each event). This time period was sufficient to capture the dynamics of the system.

Finally, the SVD-TLS Extended Prony analysis was applied to the recorded voltage signals to extract additional information on the voltage modes. The frequency signals were also analyzed in time-domain using the PFRI metric for each of the cases studied.

IV. Results and Discussion

This section presents the results from this study. First, the results from voltage stability analysis are provided. Then, the results from frequency response assessment follow.

Pursuant to the DOE Public Access Plan, this document represents the authors' peer-reviewed, accepted manuscript.
The published version of the article is available from the relevant publisher.

This article has been accepted for inclusion in a future issue of this journal. Content is final as presented, with the exception of pagination.

TABLE IV
SUMMARY OF VOLTAGE MODES FOLLOWING WIND POWER PLANT VARIABILITY

	EC01			EC02			EC03		
	Inter-area Modes	Local-area Modes	Largest Amplitude	Inter-area Modes	Local-area Modes	Largest Amplitude	Inter-area Modes	Local-area Modes	Largest Amplitude
Case 1	20	8	0.005	1	2	0.002	—	—	—
Case 2	13	9	0.005	2	—	0.002	1	—	0.002
Case 3	2	1	0.001	2	4	0.001	1	2	0.002
Case 4	3	1	0.003	2	5	0.003	1	3	0.002

Note – The numbers shown in this table indicate the number of modes identified for each case

A. Voltage Stability

In the previous section, the utility and accuracy of the SVD-TLS Extended Prony for identification of voltage modes from time-series voltage signals was established. In this section, this tool is used for small-signal voltage stability analysis of the FirstEnergy/PJM system following the variability of a 1000 MW offshore wind power plant. Due to page limitations, the detailed information of the identified voltage modes are not shown. Instead, Table IV summarizes the voltage modes for all levels of pre-disturbance wind power and magnitudes of intermittency. The modes with magnitudes less than 1×10^{-3} are neglected.

The results shown in Table IV reveal that the most significant numbers of voltage modes appear in Case 1 and Case 2 of the EC01 interconnection scenario, with the Perry online and a single interconnection at the Perry: 28 modes and 22 modes, respectively. These modes are dominantly inter-area modes: 71% and 59% of modes in Case 1 and Case 2, respectively. For the same interconnection, EC01, following the decommissioning of the Perry, the number of voltage modes reduces drastically—from 28 and 22 in Case 1 and Case 2, to 3 and 4 in Case 3 and Case 4, respectively.

The results from the EC02 interconnection scenario, with five POIs across the Lake Erie including Perry, Ashtabula, East Lake, Lake Shore, and Avon Lake, indicate up to two inter-area modes with magnitudes of less than 0.003, for each case. Additionally, the number of local-area modes in the cases with the Perry decommissioned is higher than those with the Perry online.

The results from the EC03 interconnection, with the POIs at the Lake Shore and Avon Lake exhibit absence of any oscillating mode in Case 1 and solely 1 inter-area mode with a magnitude of 0.002 in Case 2. In Case 3 and Case 4, 3 and 4 modes, respectively, are identified with a common magnitude of 0.002.

The results here point out that the integration of the offshore wind power plant through a single POI at the Perry's substation is the most sensitive, from a voltage stability perspective, to the offshore wind variability. For this interconnection scenario, the operation of the Perry causes a larger number of voltage modes at the POI following the variability of offshore wind power.

It should be noted that under the EC01 interconnection scenario, the 1000 MW wind power plant is integrated into the FirstEnergy/PJM system directly through the POI at the Perry's substation, whereas under the EC02 interconnection scenario only one-fifth of the wind power capacity, 200 MW, is integrated through this POI and the remaining 800 MW is injected into the grid through other POIs. Therefore, the inability of the online Perry to damp out the disturbances coming from the offshore power plant is more pronounced in the EC01 cases. As a result, a noticeable difference in the voltage modes among EC01, EC02, and EC03 can be observed. To explore this further, Figs. 4 and 5 compare the voltage signals from the Perry's POI, 205 with the voltage signals from the other POIs in time domain under a variety of operating conditions.

Fig. 4 compares the voltage dynamics of the POI 205, at Perry's POI, with the POI 214, at the Ashtabula's POI, in time domain for a variety of pre-disturbance levels of wind power generation. From these plots, it can be seen that the voltage dynamics at the POI 205 are a function of the pre-disturbance level of the wind power and the settling voltage varies for the difference levels of wind. At this POI, the higher the pre-disturbance level of the wind power, the greater the magnitude of voltage oscillations. At the POI 214, the voltage profiles for all pre-disturbance levels of wind power are identical and well damped out. At this POI, the settling voltage for all levels of pre-disturbance wind power is -2×10^{-4} p.u. deviated from its pre-disturbance value. The POI 205 is located in Perry at the substation of a nuclear power plant, whereas the POI 214 is located in Ashtabula at the substation of a coal-fired power plant. Thus, the neighboring generation units and the controller/stabilizer deployed in them can potentially be affecting the voltage dynamics and the oscillations caused by the wind power. This work does not have access to any detailed information regarding the power plants and their controllers and investigation of this particular effect is beyond scope of this work.

Fig. 5 compares the voltage dynamics of the POI 205, at the Perry's POI, with the POI 245, at the Avon Lake's POI, in time domain for a variety of magnitudes of wind power intermittency. These results exhibit that the voltage oscillations at the POI 245 are damped out more quickly in comparison to those at the POI 205. In both plots shown here, the settling voltage is a function of the magnitude of the wind power change; the larger the changes in the wind power, the greater the magnitude of voltage oscillations and the settling voltage. While the POI 205 is located at the Perry substation, POI 245 is located in Avon Lake at the substation of another coal-fired power plant in the area. Again, the potential effects of neighboring generation units to the POI and their controllers/stabilizers can be observed in the voltage dynamics. This agrees with the suggestions and findings in the previous paragraph of this paper.

To assess the influence of the operation of the SVC, the results from Case 1 and Case 2 should be compared to those from Case 3 and Case 4, respectively, for all three interconnections; EC01, EC02, and EC03. These results reveal that the operation of the

Pursuant to the DOE Public Access Plan, this document represents the authors' peer-reviewed, accepted manuscript.
The published version of the article is available from the relevant publisher.

This article has been accepted for inclusion in a future issue of this journal. Content is final as presented, with the exception of pagination.

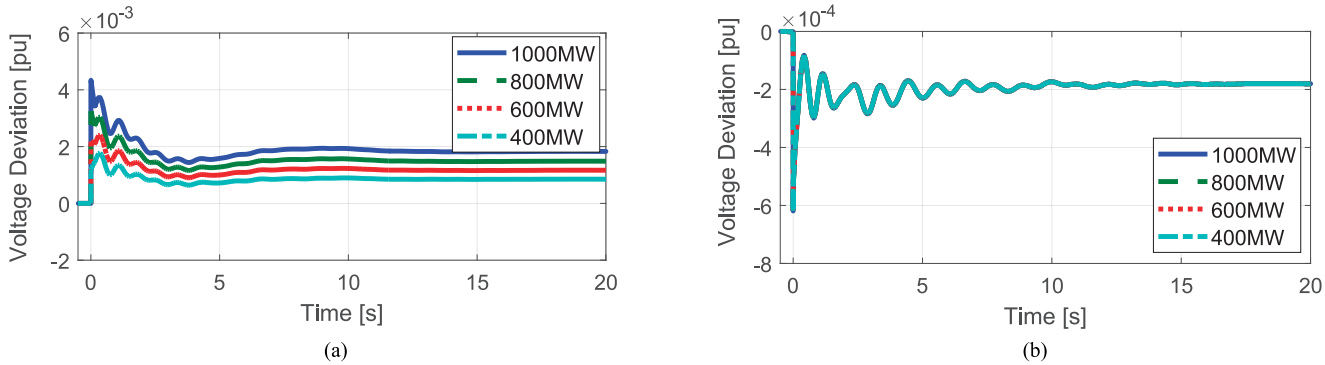

Fig. 4. Voltage signals from the POI 205 and the POI 214 following a step change in wind power for different pre-disturbance levels of wind power (a) POI 205—located at the Perry 354 kV substation. (b) POI 214—located at the Ashtabula 138 kV substation.

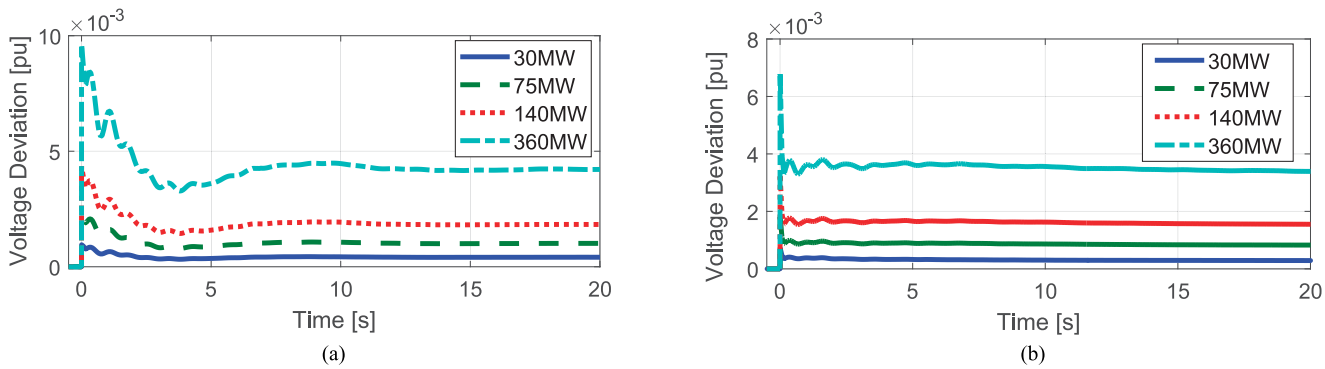

Fig. 5. Voltage signals from the POI 205 and POI 245 following different levels of change in wind power. (a) POI 205 — located at the Perry 354 kV substation. (b) POI 245—located at the Avon Lake 354 kV substation.

SVC at the POI does not significantly improve or degrade the voltage modes. The operation of the SVC, however, does slightly reduce the amplitude of the inter-area modes, but the amplitudes of the local plant modes are slightly increased.

It is worth noting that the variability of the wind power plant does not excite any interplant modes in all cases studied.

Overall, using the SVD-TLS Extended Prony, the voltage modes were successfully captured for the small-signal stability analysis of this large-scale power system in response to the variability of offshore wind power plant. The voltage modes were identified directly from the time-domain voltage measurements at the POIs. In this particular case study, for all of scenarios considered, the amplitudes of the voltage modes are very small, and their damping ratios are fairly high. Thus, it is safe to say that with the disturbances studied in this work, the FirstEnergy/PJM system retains its dynamic voltage stability after the integration of a 1000 MW offshore wind power plant.

B. Frequency Response

In the previous section, the utility and accuracy of the PFRI for frequency response assessment of power systems was established. This section presents the results from the frequency response analysis of the FirstEnergy/PJM system in response to variability of a 1000-MW offshore wind power plant. The frequency response of the offshore wind power plant was calculated in Section II as 2272 MW/0.1 Hz. The results from the events of drop and rise of the wind power are similar; therefore, to avoid repetition, the results from the rise in the level of wind power generation are not shown.

Fig. 6 shows the computed values of the PFRI metric for the cases studied. These results reveal that the FirstEnergy/PJM system's frequency response under the EC01 interconnection in those cases with the Perry decommissioned (Case 3 and Case 4), single POI at the Perry's substation, the frequency response is within the standard range, between 2223 and 2586 MW/0.1 Hz, whereas under the same interconnection, EC01, in those cases with Perry online (Case 1 and Case 2), the frequency response is nearly halved, ranging between 1034 and 1163 MW/0.1 Hz. Meanwhile, for all cases studied under the EC02 and EC03 interconnections, the frequency response remains within the standard range of 2086–2777 MW/0.1 Hz. This suggests that while the offshore wind power plant is solely integrated through the Perry's substation, the operation of this power plant degrades the frequency response of the system.

Fig. 7 compares the area frequency in time domain for the two cases, with and without Perry, under the EC01 and EC02 interconnection scenarios. These results show that the frequency swings in the EC01 cases are nearly doubled for the cases with Perry online as compared to the other cases with Perry decommissioned. The results from the EC02 exhibit a very consistent area frequency response regardless of the operational

Pursuant to the DOE Public Access Plan, this document represents the authors' peer-reviewed, accepted manuscript.
The published version of the article is available from the relevant publisher.

This article has been accepted for inclusion in a future issue of this journal. Content is final as presented, with the exception of pagination.

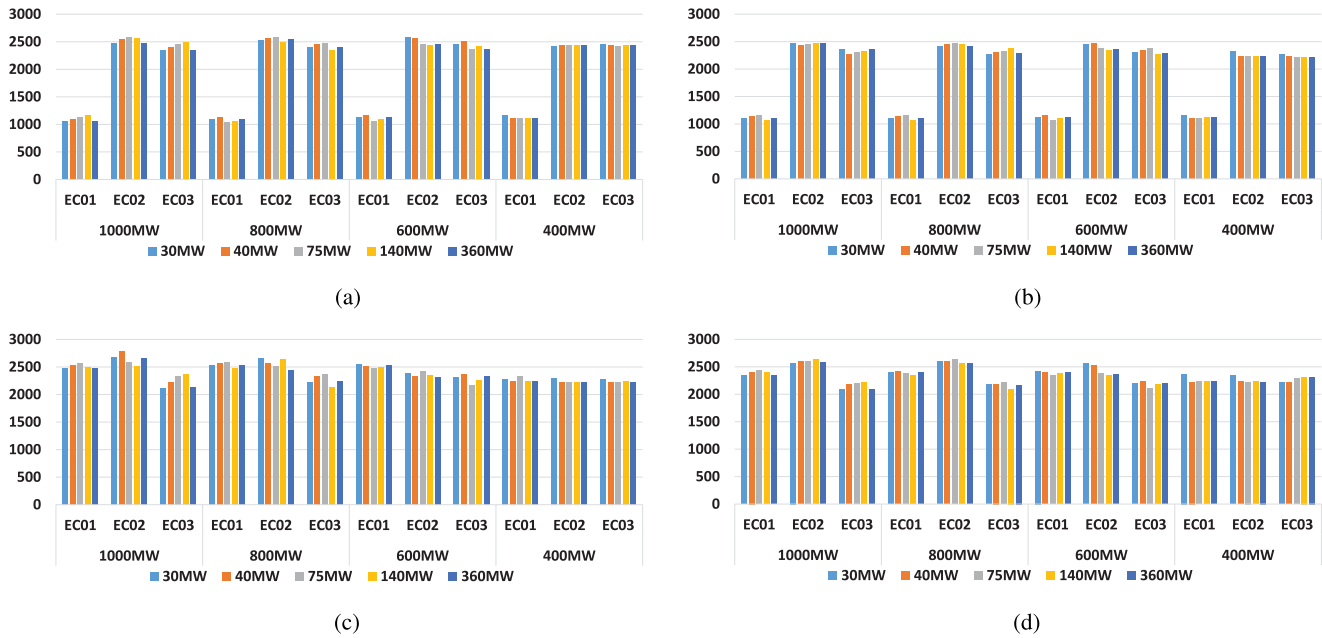

Fig. 6. PFRI values for the wind power generation drop. (a) Case 1 - Perry Online - SVC Offline. (b) Case 2 - Perry Online - SVC Online. (c) Case 3 - Perry Offline - SVC Offline. (d) Case 4 - Perry Offline - SVC Online.

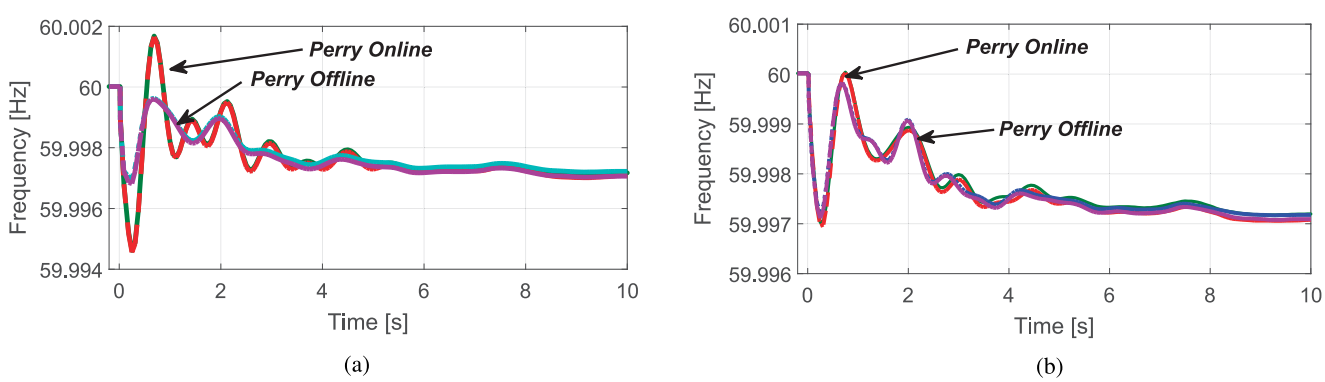

Fig. 7. Primary frequency response in the FirstEnergy area to 140 MW drop in level of wind power generation for EC01 and EC02 interconnections. (a) EC01, single POI at Perry, (b) EC02, five POIs across the Lake Erie at Perry, Ashtabula, East Lake, Lake Shore, and Avon Lake.

status of the Perry. These results highlight the importance of the operational status of Perry under the EC01 interconnection scenario.

In order to understand the effects of the operation of the SVC on the frequency response of the system, the results from Case 1 and Case 3 should be compared with those from Case 2 and Case 4, respectively. The results here outline that, under all three interconnection scenarios considered here, EC01, EC02, and EC03, the operation of the SVC at the POIs does not have any significant effect on the system's frequency response. Hence, frequency response remains independent from the operation of the SVC.

Fig. 8 illustrates the relationship among the size of the change in level of wind power, the pre-disturbance level of the offshore wind power generation, and the nadir and settling frequencies of the system. These results show that the nadir frequency is a function of the level of drop in wind power generation; the higher the magnitude of change in wind power, the lower the nadir frequency. They also point out that the settling frequency is a function of the level of wind power changes; the greater the level of rise or drop, the larger the deviation in steady-state frequency from the 60.00 Hz set point. However, the pre-disturbance level of power generation by the offshore wind plant does not affect the frequency response.

In all cases studied here, following the wind variability, the nadir frequency remains above the Eastern Interconnection's under-frequency load shedding (UFLS) threshold for all levels of change and all pre-disturbance operating points of the offshore wind power plant. The lowest nadir frequencies recorded are 59.975 Hz following a 360-MW wind power drop and 59.992 Hz following a 360-MW wind power rise. According to the North American Electric Reliability Corporation UFLS

Pursuant to the DOE Public Access Plan, this document represents the authors' peer-reviewed, accepted manuscript. The published version of the article is available from the relevant publisher.

This article has been accepted for inclusion in a future issue of this journal. Content is final as presented, with the exception of pagination.

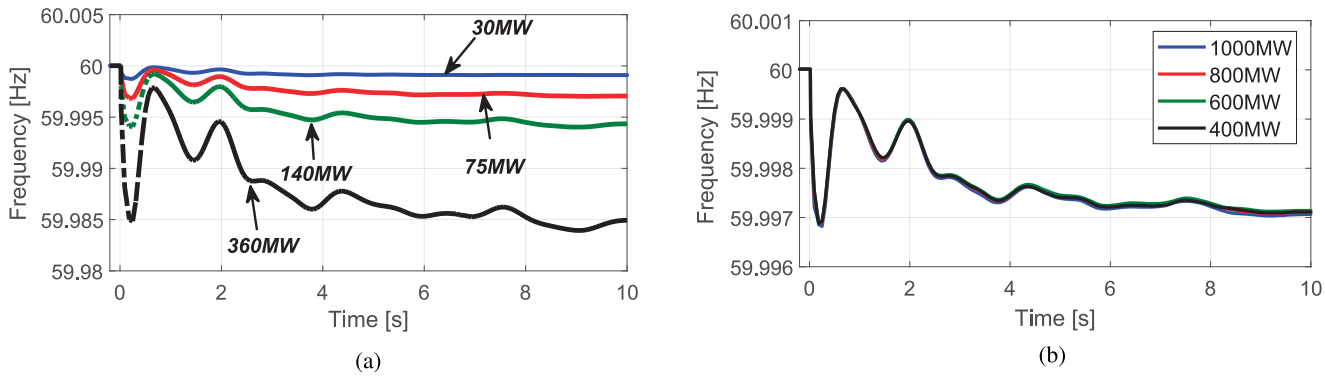

Fig. 8. Primary frequency response in the FirstEnergy area to drop in offshore wind power generation for EC01 the interconnection. (a) Different levels of wind power drop at a given pre-drop operating point of the offshore wind power plant. (b) Different pre-drop operating points of the offshore wind power plant at a given level of wind power drop.

reliability standard in the Eastern Interconnection, the UFLS threshold for generators with 100 MW or more of peak net load must be set at 59.50 Hz [31].

Overall, using the PFRI metric, the frequency response of this large-scale power system in response to variability of wind power generation was successfully assessed. Regarding this particular case study; the results show the ability of the FirstEnergy/PJM system to arrest the frequency fluctuations within the first 10 s following a drop or rise in the level of power generation by the offshore wind power plant. For all of cases studied, the nadir frequencies are well above the UFLS threshold of the Eastern Interconnection.

V. Conclusion

This paper presented a methodology for a small-signal stability analysis of large-scale power systems in response to the variability of offshore wind power plants. This methodology includes an SVD-TLS Extended Prony analysis for deriving voltage modes directly from the time-domain measurement of voltage signals. Additionally, the PFRI is presented and used to assess frequency response of the system following intermittency of wind power. The computational nature of these tools increases their utility in large-scale system planning studies. They are easy to implement on existing practical network models that include the effects of continuous and discontinuous system elements, in all available power system planning and simulation packages.

The integration of a 1000 MW offshore wind power plant operating in Lake Erie into FirstEnergy/PJM service territory was considered as a case study. A simulation model of the U.S. Eastern Interconnection, an approximately 63 000-bus test system, was used in GE's PSLF software package. The results demonstrated the application and accuracy of the proposed methodology. They also revealed that the FirstEnergy/PJM system retains its dynamic stability after the integration of this offshore wind power plant.

Moreover, in this paper, it was observed that voltage and frequency oscillations are affected by the neighboring generation units and the controller/stabilizer used in those units. Hence, additional work is required to completely comprehend how operation of generation units, which are located close to the POIs of the offshore wind power plants, and their controller schemes can affect the dynamics and control of the grid and the offshore wind power plants.

Acknowledgment

The authors would like to thank R. Kolacinski from the Case Western Reserve University and S. Barnes and R. D'Aquila from the General Electric for their assistance.

References

[1] J. Machowski, J. Bialek, and J. Bumby, *Power System Dynamics: Stability and Control*. New York, NY, USA: Wiley, 2008.

[2] A. Sajaid, R. Preece, and J. Milanovic, "Evaluation of suitability of different transient stability indices for identification of critical system states," in *Proc. 10th Bulk Power Syst. Dyn. Control Symp.*, Espinho, Portugal, pp. 1–7, 2017.

[3] J. Narain, "Turbines turned off... because it's too windy! they automatically shut down as gusts of 85 mph swept country," 2015, [Online]. Available: https://www.dailymail.co.uk/news/article-3324722/Turbines-turned-s-windy-automatically-shut-gusts-85mph-swept-country.html.

[4] I. Dobson, H. Glavitsch, C.-C. Liu, Y. Tamura, and K. Vu, "Voltage collapse in power systems," *IEEE Circuits Devices Mag.*, vol. 8, no. 3, pp. 40–45, May 1992.

[5] M. Jafarian and A. M. Ranjbar, "Interaction of the dynamics of doubly fed windgenerators with power system electromechanical oscillations," *IET Renew. Power Gener.*, vol. 7, no. 2, pp. 89–97, 2013.

[6] Y. Mishra, S. Mishra, F. Li, Z. Y. Dong, and R. C. Bansal, "Small-signal stability analysis of a DFIG-based wind power system under different modes of operation," *IEEE Trans. Energy Convers.*, vol. 24, no. 4, pp. 972–982, Dec. 2009.

[7] K. R. Padiyar and K. Bhaskar, "Analysis of small signal voltage stability in multimachine systems using detailed and reduced formulations," *Int. J. Electr. Power Energy Syst.*, vol. 27, no. 4, pp. 301–317, 2005.

[8] J. F. Hauer, C. Demeure, and L. Scharf, "Initial results in Prony analysis of power system response signals," *IEEE Trans. Power Syst.*, vol. 5, no. 1, pp. 80–89, Feb. 1990.

[9] J. Hauer, "Application of Prony analysis to the determination of modal content and equivalent models for measured power system response," *IEEE Trans. Power Syst.*, vol. 6, no. 3, pp. 1062–1068, Aug. 1991.

[10] M. Johnson, I. Zarafonitis, and M. Calligaris, "Prony analysis and power system stability-some recent theoretical and applications research," in *Proc. IEEE Power Eng. Soc. Summer Meeting*, 2000, vol. 3, pp. 1918–1923.

[11] D. N. Kosterev, C. W. Taylor, and W. A. Mittelstadt, "Model validation for the August 10, 1996 wscc system outage," *IEEE Trans. Power Syst.*, vol. 14, no. 3, pp. 967–979, Aug. 1999.

[12] E. Muljadi, V. Gevorgian, M. Singh, and S. Santoso, "Understanding inertial and frequency response of wind power plants," in *Proc. IEEE Power Electron. Mach. Wind Appl.*, 2012, pp. 1–8.

Pursuant to the DOE Public Access Plan, this document represents the authors' peer-reviewed, accepted manuscript. The published version of the article is available from the relevant publisher.

This article has been accepted for inclusion in a future issue of this journal. Content is final as presented, with the exception of pagination.

[13] Y. Zhang, J. Bank, Y.-H. Wan, E. Muljadi, and D. Corbus, "Synchrophasor measurement-based wind plant inertia estimation," in *Proc. IEEE Green Technol. Conf.*, 2013, pp. 494–499.

[14] S. Barnes, "Progress report - great lakes offshore wind: Utility and regional integration study," Tech. Rep., General Electric, Pittsburgh, PA, USA, 2014.

[15] N. Miller, M. Shao, S. Pajic, and R. DAquila, "Eastern frequency response study," *Contract*, vol. 303, pp. 275–3000, 2013.

[16] N. Miller, M. Shao, S. Pajic, and R. DAquila, "Eastern frequency response study," Tech. Rep. NREL/SR-5500-58077, Nat. Renew. Energy Lab., Golden, CO, USA, 2013.

[17] N. W. Miller, W. W. Price, and J. J. Sanchez-Gasca, "Dynamic modeling of ge1.5 and 3.6 wind turbine-generators," *GE-Power Systems Energy Consulting*, 2003.

[18] S. L. Marple, *Digital Spectral Analysis: With Applications*, vol. 5. Englewood Cliffs, NJ, USA: Prentice-Hall, 1987.

[19] Y. Zhao, Y. Gao, Z. Hu, Y. Yang, J. Zhan, and Y. Zhang, "A new method of identifying the low frequency oscillations of power systems," in *Proc. Int. Conf. Energy Environ. Technol.*, 2009, vol. 2, pp. 19–22.

[20] J. Xiao, X. Xie, Y. Han, and J. Wu, "Dynamic tracking of low-frequency oscillations with improved prony method in wide-area measurement system," in *Proc. Power Eng. Soc. General Meeting*, 2004, pp. 1104–1109.

[21] J. A. Cadzow, "Spectral estimation: An overdetermined rational model equation approach," *Proc. IEEE*, vol. 70, no. 9, pp. 907–939, Sep. 1982.

[22] P. M. Anderson and A. A. Fouad, *Power System Control and Stability*. New York, NY, USA: Wiley, 2008.

[23] P. W. Sauer and M. Pai, *Power System Dynamics and Stability*. New York, NY, USA: Wiley, 1998.

[24] NERC, "Frequency Response Standard Background Document," North Amer. Elect. Rel. Corp., Princeton, NJ, USA, 800 Tech. Rep., 2012, [Online]. Available: https://www.nerc.com/pa/Stand/Project%20200712%20Frequency%20Response%20DL/Bal-003-1-Background_Document-Clean-2013_FILING.pdf.

[25] P. Mackin, "Dynamic simulation studies of the frequency response of Three US interconnections with increased wind generation," Lawrence Berkeley Nat. Lab., Berkeley, CA, USA, 2011.

[26] J. H. Eto, "Use of frequency response metrics to assess the planning and operating requirements for reliable integration of variable renewablegeneration," Lawrence Berkeley Nat. Lab., Berkeley, CA, USA, 2011.

[27] "Rate of Change of Frequency (ROCOF) withstand capability," Tech. Rep., European Network of Transmission System Operators for Electricity, Bruxelles, Belgium, 2017, [Online]. Available: https://docstore.entsoe.eu/Documents/Network%20codes%20documents/NC%20RfG/IGD_RoCoF_withstand_capability_final.pdf.

[28] G. Kou, M. Till, T. Bilke, S. Hadley, Y. Liu, and T. King, "Primary frequency response adequacy study on the us eastern interconnection under high-wind penetration conditions," *IEEE Power Energy Technol. Syst. J.*, vol. 2, no. 4, pp. 125–134, Dec. 2015.

[29] ABB, "Submarine cable systems: Attachment to XLPE land cable systems-users guide," 2010.

[30] S. Barnes, R. D'Aquila, and B. Thomas, "GE PSLF User Manual," Tech. Rep., General Electr., Schenectady, NY, USA, 2011.

[31] J. Mackauer, J. Syner, P. Bowers, and J. Detweiler, "FirstEnergy/PJM requirements for transmission connected facilities," Tech. Rep., First Energy, Akron, OH, USA, 2013, [Online]. Available: https://www.firstenergycorp.com/content/dam/feconnect/files/wholesale/Requirements-for-Transmission-Connected-Facilities-10-03-2016.pdf.

Amirhossein Sajadi (S'12–M'16) received the Ph.D. degree in systems and control engineering from the Case Western Reserve University, Cleveland, OH, USA, in 2016.

He is a Research Associate with the Department of Electrical Engineering and Computer Science, Case Western Reserve University. His main research includes modeling, planning, optimization, real-time control, stability and management of large scale power systems, including renewable sources and microgrid to enhance the stability, security, and resiliency of energy delivery.

Shuang Zhao received the B.E. degree in automation from Nanchang University, Nanchang, China, in 2007 and the Ph.D. degree in systems and control engineering from Case Western Reserve University, Cleveland, OH, USA, in 2017.

Her research interests include statistical signal processing, parameter estimation, and their applications in electric power systems.

Kara Clark (F'12) received the BSEE degree from the University of Colorado, Boulder, CO, USA, in 1984, and the M.Sc. degree in electrical power engineering from the Rensselaer Polytechnic Institute, Troy, NY, USA, in 1987.

She is retired from the National Renewable Energy Laboratory (NREL), Golden, CO, USA, where she worked on the issues related to the integration of significant levels of wind and solar generation into the bulk transmission system. She led Phase 3 of the Western Wind and Solar Integration Study, which analyzed frequency response and transient stability with high renewable penetration. Prior to joining NREL, she was with GE, where she was a principal contributor to many of the key U.S. wind integration studies and the development of dynamic models of wind and solar plants.

Kenneth A. Loparo (F'99–LF'16) received the Ph.D. degree in systems and control engineering from Case Western Reserve University, Cleveland, OH, USA, in 1977.

He is the Arthur L. Parker Professor with the Department of Electrical Engineering and Computer Science and the Faculty Director of the Institute for Smart, Secure and Connected Systems, Case Western Reserve University. His research interests include stability and control of nonlinear and stochastic systems with applications to large-scale electricity systems including generation and transmission and distribution; nonlinear filtering with applications to monitoring, fault detection, diagnosis, prognosis and reconfigurable control; information theory aspects of stochastic and quantized systems with applications to adaptive and dual control and the design of distributed autonomous control systems.

Pursuant to the DOE Public Access Plan, this document represents the authors' peer-reviewed, accepted manuscript. The published version of the article is available from the relevant publisher.